PROCEEDINGS OF THE INTERNATIONAL CONFERENCE NANOMATERIALS: APPLICATIONS AND PROPERTIES
Vol. **2** No 3, 03NCNN12(4pp) (2013)

Car-Parrinello Molecular Dynamics of Nanosized Graphene Sheets

S.Q. Wang*

Shenyang National Laboratory for Materials Science, Institute of Metal Research, Chinese Academy of Sciences, Shenyang 110016, China

(Received 19 May 2013; published online 30 August 2013)

Car-Parronello molecular dynamics simulations of twelve nanosized graphene sheets with a dozen to a hundred carbon atoms are performed using a mixed Gaussian and planewave approach within the framework of the density-functional theory. Two different origins for the rippled structure of graphene are found: the thermodynamic vibration of atoms and the local lattice defect. We suggest that the lattice defect, which changes the local atomic bonding state, should be responsible for the intrinsic ripples in graphene sheet.

Keywords: Graphene, Rippled structure, Nano-sheets, CPMD, DFT.

PACS number(s): 61.46.-w, 71.15.Pd

1. INTRODUCTION

The discovery of graphene [1] ended the long-standing theoretical debate on the possibility for the existence of two-dimensional (2D) materials. In addition to graphene, several other 2D phases were also theoretically suggested [2] and experimentally prepared, including silicene [3], the 2D monolayers of BN[4] and SiC [5]. Graphene is the only one that had successfully prepared in the free-stand state without a substrate support among of all these 2D phases so far. The intrinsic ripples was observed in the suspended graphene sheets [6], and the reason for these ripples is being involved another hot debate at present [7-10]. These are both the localized sp^2 and non-localized π bonds in graphene sheet [11]. There are three resonance π bonds arranged at regular intervals in a hexagonal C-ring of graphene monolayer in ideal case. It is possible that the collective effect of π-bonds could cause the local lattice distortion, and hence leads to the intrinsic ripples in graphene. In addition to this, the situation of atomic bonding around lattice defect is much more complicated, all of the sp, sp^2, and sp^3 bonds could be present. Unfortunately, most of the reported theoretical works on this problem were merely done by atomistic simulation without sufficient consideration of the bonding variations.

We present a set of comparative Car-Parrinello Molecular Dynamics (CPMD) simulations of different nanosized graphene sheets under finite temperature to investigate the effect of local chemical bondings to the geometry of these graphene sheets using CP2K code [12]. The local lattice distortion and the therm-?dynamically stable sheet configuration for each of these cases are analysed in details. Our research result reveals a close correlation between the intrinsic ripples and structure defects in graphene phase.

2. MODEL BUILDING AND CALCULATION DETAILS

2.1 Model building of graphene nano-sheets

We build twelve models of nanosized graphene sheet with atoms up to 126 atoms in this work. These models are divided into four types. The models of Type-I are the $n\times n$ (n=3, 5, 7) cells directly cut from a large piece of graphene sheet. There are some carbon atoms without in the C_6-ring structure. These models are C_{18}, C_{50}, and C_{98} as illustrated in Figs. 1 (a), (e) and (i). Type-II models are the hydrogenated Type-I ones, *i.e.*, $C_{18}H_{12}$, $C_{50}H_{20}$, and $C_{98}H_{28}$ as shown in Figs. 1 (b), (f) and (j). The Type-III models, C_{16}, C_{48}, and C_{96} are created by deleting the carbon atoms without forming C_6-ring structure in Type-I models as given in Figs. 1 (c), (g) and (k). Figs. 1 (d), (h) and (l) present the Type-IV models ($C_{16}H_{10}$, $C_{48}H_{18}$, and $C_{96}H_{26}$) which just are the corresponding hydrogenated Type-III models. There are plentiful variations of local atomic bonding in these models and thus are very suitable for investigation of the chemical bonding factor to the geometry structure of nanosized graphene sheets.

2.2 Details of Car-Parrinello Molecular Dynamics Simulation

The periodic boundary condition is used in our CPMD simulation. Each of the nanosized graphene sheets created in section 2.1 is positioned at the center of a cuboid box with at least 5Å away to the inner surface of the box along each direction. The non-bonding distance between carbon-hydrogen is smaller than that between carbon-carbon. The largest bonding distance between carbon-carbon is about 2.38Å [11]. Therefore, the above supercell dimension is good enough for establishing the environment of spatially isolated nanosized graphene sheets.

The Quickstep algorithm by a mixed Gaussian and planewave approach is adopted in our Car-Parrinello simulation [13]. The valence electrons are treated with double Z valence and one polarization function optimized for the Goedecker-Teter-Hutter (GTH) pseudopotential and the LDA Teter and Pade exchange-correlation functional. The effect of core electrons and nuclei are represented using norm-conserving GTH pseudopotentials [14,15]. A 280Ry energy cutoff is

* sqwang@imr.ac.cn

adopted in CPMD simulation. The system temperature increases from 0K to 300K through three stages by the Nose-Hoover thermostat technique. 20000 MD steps are performed for each model with the time-step 0.5fs, which accounts total 10ps in a MD run.

3. RESULTS AND ANALYSES

The atomic coordinates and energy information are recorded for each MD step. The system temperature, total kinetic and potential energies for all the model systems reach the state of convergence when the simulation is completed. In the follows, we perform comparative analyses for the structural evolutions of these models during the simulation by grouping them into small, medium, and large nanosized sheets according to the three horizontal rows in Fig. 1.

3.1 Small graphene sheets

There are four structure configurations in this group: C_{18}, $C_{18}H_{12}$, C_{16} and $C_{16}H_{10}$. Our simulated results show that there are three nano-sheets, C_{18}, C_{16} and $C_{16}H_{10}$ which are thermodynamic unstable structures. The finally atomic configurations after 20000 MD steps for these nano-sheets are presented in Fig. 2.

C_{16} nano-sheet is the most unstable in these models. The C_6-rings break soon in few hundred MD steps for C_{16} model. The nano-sheet finally evolves to a mixed structure with a C_3- and a C_4-rings connected by short carbon chains (Fig. 2(c)). This local structural characteristic is consist with the previous DFT ground-state calculation [16]. However, the C_{18} model with two dangling carbon atoms is more stable than C_{16}: each of the two C_6-rings connected with the two dangling-C in Fig. 1(a) loses a carbon atom and changes two C_5-rings in a few hundred MD steps. Then these two C_5-rings exchange positions with the remaining two C_6-rings at the cluster center. The final stabilized C_{18} nano-sheet is given in Fig. 2(a). Some hydrogen bonding is quite weak in $C_{16}H_{10}$ sheet. The cluster loses four hydrogen atoms and becomes $C_{16}H_6$ soon after the simulation starts. But, the $C_{16}H_6$ sheet is very stable and keeps its configuration to the end of the simulation (Fig. 2(d)). $C_{18}H_{12}$ is very thermodynamically stable. It has no obvious configurational change throughout the whole simulation (Fig. 2(b)), only small off sheet-plane fluctuations of the carbon atoms are observed.

3.2 Medium graphene sheets

The four nano-sheets of medium size in this study are C_{50}, $C_{50}H_{20}$, C_{48}, and $C_{48}H_{18}$ as given in Figs. 1(e) to (h). There are two dangling carbon atoms in C_{50}. The local structure evolution near these dangling-C atoms are as follows. Firstly, the nearest C_6-ring to the dangling-C changes to a C_5-ring and a C_3-ring. Then, the dangling-C joins with C_3-ring to form a C_4-ring. This sheet configuration keeps until the end of simulation. There are significant local structure distortion and bending near the C_4- and C_5-rings as shown in Fig. 2(e). Although $C_{50}H_{20}$ is structurally stable (Fig. 2(f)), a regular lattice fluctuation vertical to the sheet-plane is observed during the simulation. The fact indicates that the vertical lattice vibration must be an important factor for the ripples in graphene sheets. However as shown in present work, this kind of thermal fluctuations varies with time. In contrast with C_{16}, the C_{48} nano-sheet without any dangling-C keeps its original configuration steadily during the simulation with only very small vertical fluctuation is observed. The MD result for $C_{48}H_{18}$ is similar to $C_{50}H_{20}$, the obvious structural variation is only the lattice fluctuation caused by temperature.

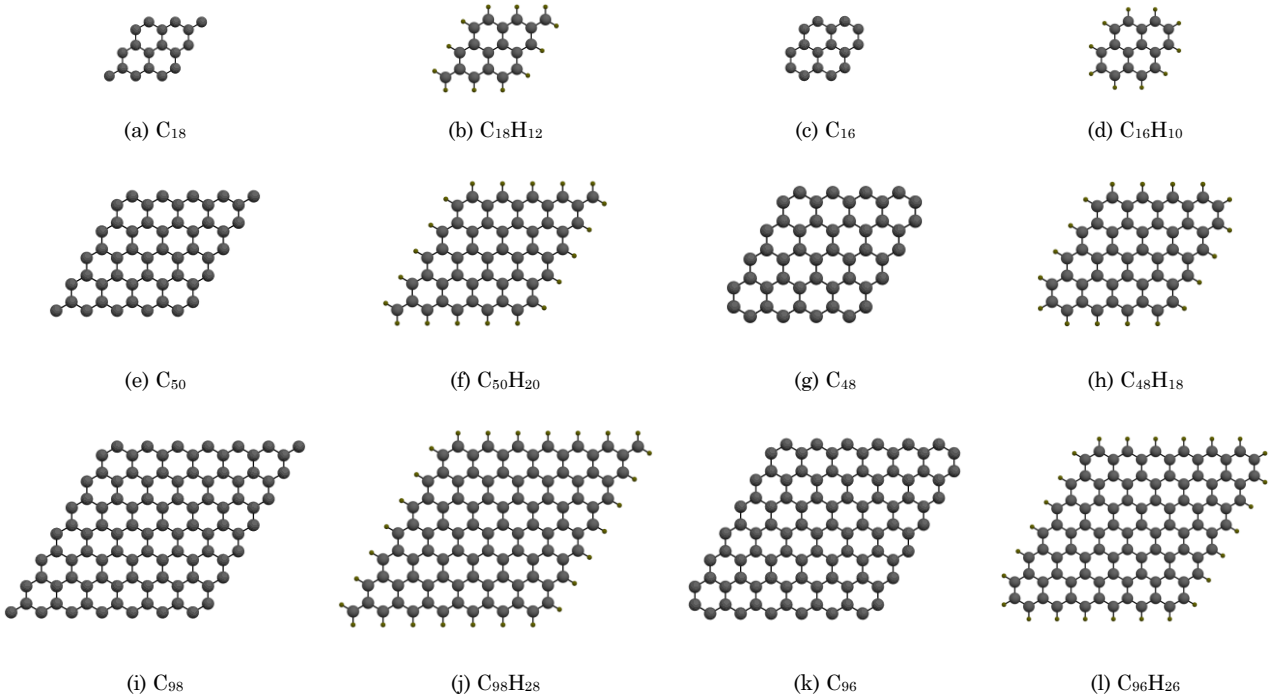

Fig. 1 – Atomic structure models of nanosized graphene sheets. The carbon and hydrogen atoms are represented by big and small balls, respectively.

3.3 Large graphene sheets

All the four large graphene sheets, C_{98}, $C_{98}H_{28}$, C_{96}, $C_{96}H_{26}$, are comparatively more stable than those small ones in this study. There is no significant configurational change except the thermal fluctuation for last three models throughout the whole simulation (Fig. 2(j)-(l)). Just the same as in the previous simulation, some structural change is seen for C_{98} due to the dangling-C atoms in this model. Our simulated result shows that these high-energy dangling-C local structures turn into the C_3-rings in a few hundred steps after the simulation starts (Fig. 2(i)). This structure change causes large local lattice distortion in the two acute-angle areas of C_{98}. The lattice distortions are gradually smoothened and spread to the whole sheet. This phenomenon finally conducts to a global structure bending of the C_{98} sheet.

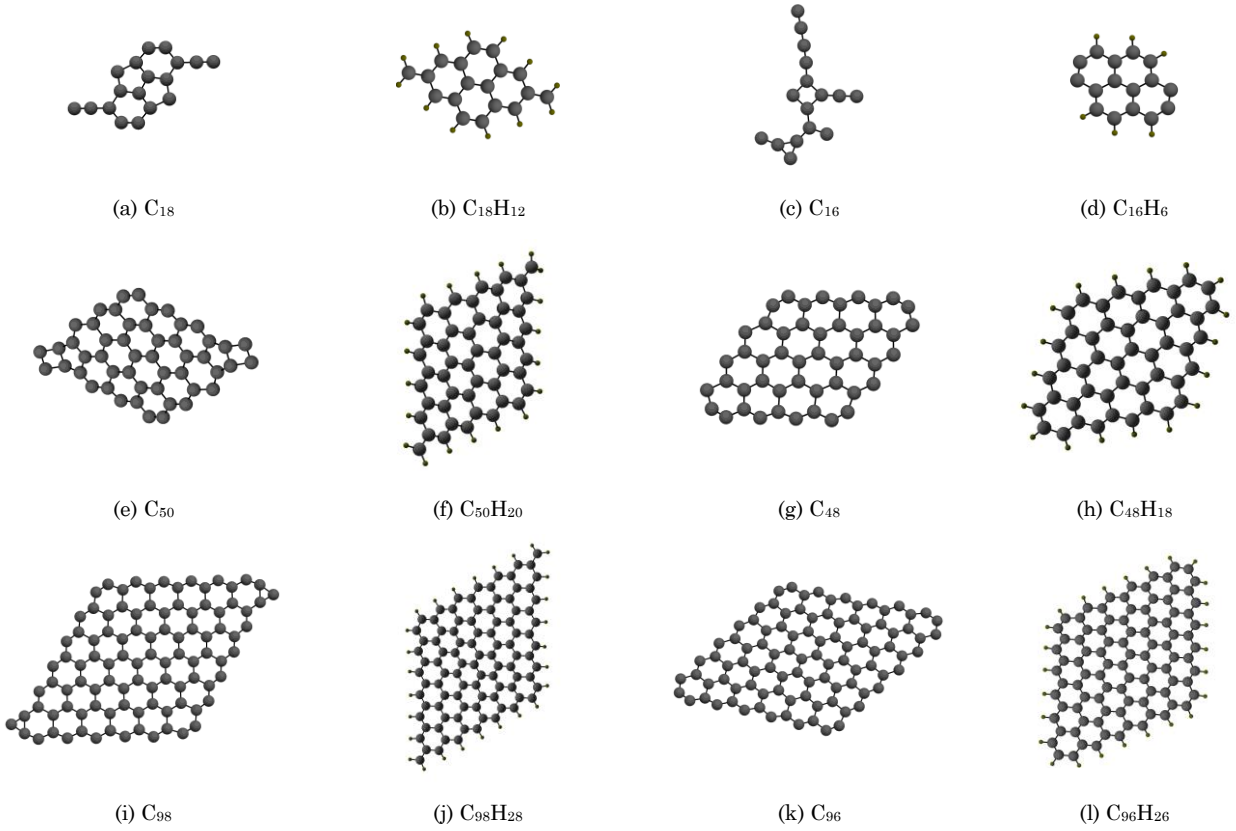

(a) C_{18} (b) $C_{18}H_{12}$ (c) C_{16} (d) $C_{16}H_6$

(e) C_{50} (f) $C_{50}H_{20}$ (g) C_{48} (h) $C_{48}H_{18}$

(i) C_{98} (j) $C_{98}H_{28}$ (k) C_{96} (l) $C_{96}H_{26}$

Fig. 2 – Atomic structure models of nanosized graphene sheets after 20000 CPMD steps. The carbon and hydrogen atoms are represented by big and small balls, respectively.

4. DISCUSSIONS

4.1 Thermodynamic structure stability of nano-sized graphene sheets

From the results of present Car-Parrinello molecular simulation, the following general rules for the thermodynamic structure stability of nano-sized graphene sheets can be summed up. Those very small graphene sheets with only a dozen carbon atoms are thermodynamic unstable because there are no enough electrons to form π-bonding to stabilize the C_6-rings in these models. These sheets will evolve to the mixed structures by chains and small C-rings (C_3-ring, C_4-ring, C_5-ring) by carbon atoms. However, the hydrogenated small graphene sheets are structurally very stable. The reason is that the electrons from hydrogen atoms saturate the unfilled electronic orbits, which reduce the total system energy.

Those configurations without dangling-C is more stable for larger graphene sheets. The dangling-C configuration can be stabilized by forming smaller carbon rings, such as in C_{50} and C_{98}, in the nano-sized graphene sheets with dangling carbon atoms. However, obvious lattice distortion will be caused by this kind of structure change. All the hydrogenated larger graphene sheets are thermodynamically very stable.

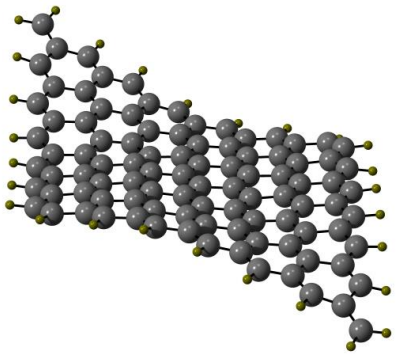

Fig. 3 – Rippled $C_{98}H_{28}$ nano-sheet by atomic thermodynamic movement

4.2 Origin of the rippled structure in graphene sheet

Two different origins for the ripples in graphene sheets are found based on the results from the present study. Firstly, the atomic plane bending due to the thermodynamic motion of atoms is observed in all these models. This is the lattice fluctuation by temperature. In this case, the ripples move much fast and their dimensions are in proportional to the temperature. The example ripple structure of this type for $C_{98}H_{28}$ sheet is illustrated in Fig. 3. The degree of the ripples by this reason is quite small when temperature is lower than 100K.

The second origin of ripples in graphene sheets comes from the chemical bonding variation due to local lattice defects. As seen in the cases of C_{50} and C_{98}, the mode of atomic bonding is changed by local non-C_6 carbon-ring configurations at the acute-angle corners of these sheets. This change causes the lattice plane bent initiated at these corner areas. These local bent areas gradually expand and merge together with time goes, and finally it leads to the rippled structure of the whole sheet. Compared to the first origin, the extent of the ripples by structure defects is relatively large. These ripples change much slowly, and they will not disappear even at 0K. The ripple structure evolution of this type for C_{98} is presented in Fig. 4(a) to (c). We suggest that the intrinsic ripples in graphene sheets should be basically arisen from lattice defects. The ripples created by temperature are intrinsic.

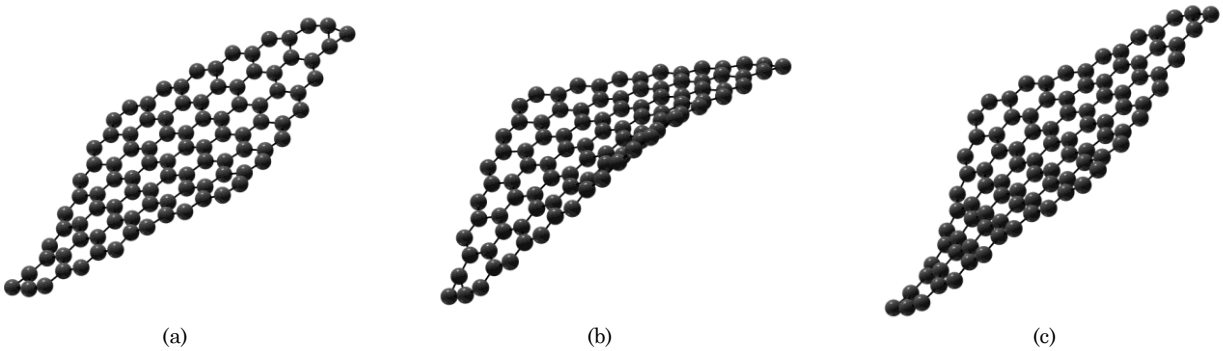

(a) (b) (c)

Fig. 4 – Evolution of the rippled structure in C_{98} graphene sheet.

5. CONCLUSIONS

Car-Parrinello molecular dynamics simulations for nanosized graphene sheets are performed for investigating the origin of the rippled structure in the materials. Our results show that the change in chemical bonding due to local lattice defect is the root cause of the intrinsic ripples in graphene sheet.

AKNOWLEDGEMENTS

This work was supported by the National Basic Research Program of China (No. 2011CB606403) and the National Natural Science Foundation of China (No. 51071149).

REFERENCES

1. K. S. Novoselov, A. K. Geim, *et al.*, *Science* **306,** 666 (2004).
2. S. Q. Wang, *J. Phys. Soc. Jpn.* **79,** 064602 (2010).
3. P. D. Padova, C. Quaresima, *et al.*, *Appl. Phys. Lett.*, **96,** 261905 (2010).
4. D. Golberg, Y. Bando, *et al.*, *ACS Nano* **4**, 2979 (2010).
5. Y. Baba, T. Sekiguchi, *et al.*, *Appl. Surf. Sci.* **237,** 176 (2004).
6. J. C. Meyer, A. K. Geim, *et al.*, *Nature* **446,** 60 (2007).
7. A. Fasolino, J. H. Los, *et al.*, *Nature Mater.* **6,** 858 (2007).
8. R. C. Thompson-Flagg, M. J. B. Moura, *et al.*, *EPL* **85,** 46002 (2009).
9. Z. Wang and M. Devel, *Phys. Rev. B* **83,** 125422 (2011).
10. P. San-Jose, J. Gonzalez, and F. Guinea, *Phys. Rev. Lett.* **106,** 045502 (2011).
11. S. Q. Wang, *Chem. Phys. Phys. Chem.* **13,** 11929 (2011).
12. http://www.cp2k.org/.
13. J. VandeVondele, M. Krack, F. Mohamed, M. Parrinello, T. Chassaing and J. Hutter, *Comp. Phys. Comm.* **167**, 103 (2005).
14. S. Goedecker, M. Teter, and J. Hutter, *Phys. Rev. B* **54**, 1703 (1996).
15. C. Hartwigsen, S. Goedecker, and J. Hutter, *Phys. Rev. B* **58**, 3641 (1998).
16. R. O. Jones, *J. Chem. Phys.* **110**, 5189 (1999).